



ALMA MATER STUDIORUM  
UNIVERSITÀ DI BOLOGNA

ARCHIVIO ISTITUZIONALE  
DELLA RICERCA

## Alma Mater Studiorum Università di Bologna Archivio istituzionale della ricerca

Chitosan-pectin hybrid nanoparticles prepared by coating and blending techniques

This is the final peer-reviewed author's accepted manuscript (postprint) of the following publication:

*Published Version:*

Rampino A., Borgogna M., Bellich B., Blasi P., Virgilio F., Cesaro A. (2016). Chitosan-pectin hybrid nanoparticles prepared by coating and blending techniques. EUROPEAN JOURNAL OF PHARMACEUTICAL SCIENCES, 84, 37-45 [10.1016/j.ejps.2016.01.004].

*Availability:*

This version is available at: <https://hdl.handle.net/11585/703589> since: 2020-02-25

*Published:*

DOI: <http://doi.org/10.1016/j.ejps.2016.01.004>

*Terms of use:*

Some rights reserved. The terms and conditions for the reuse of this version of the manuscript are specified in the publishing policy. For all terms of use and more information see the publisher's website.

This item was downloaded from IRIS Università di Bologna (<https://cris.unibo.it/>).  
When citing, please refer to the published version.

(Article begins on next page)

This is the final peer-reviewed accepted manuscript of: **Antonio Rampino, Massimiliano Borgogna, Barbara Bellich, Paolo Blasi, Francesca Virgilio and Attilio Cesàro. Chitosan-pectin hybrid nanoparticles prepared by coating and blending techniques. European Journal of Pharmaceutical Sciences 84 (2016) 37–45.**

The final published version is available online at:  
<https://www.sciencedirect.com/science/article/pii/S0928098716300045?via%3Dihub#:~:text=https%3A//doi.org/10.1016/j.ejps.2016.01.004>

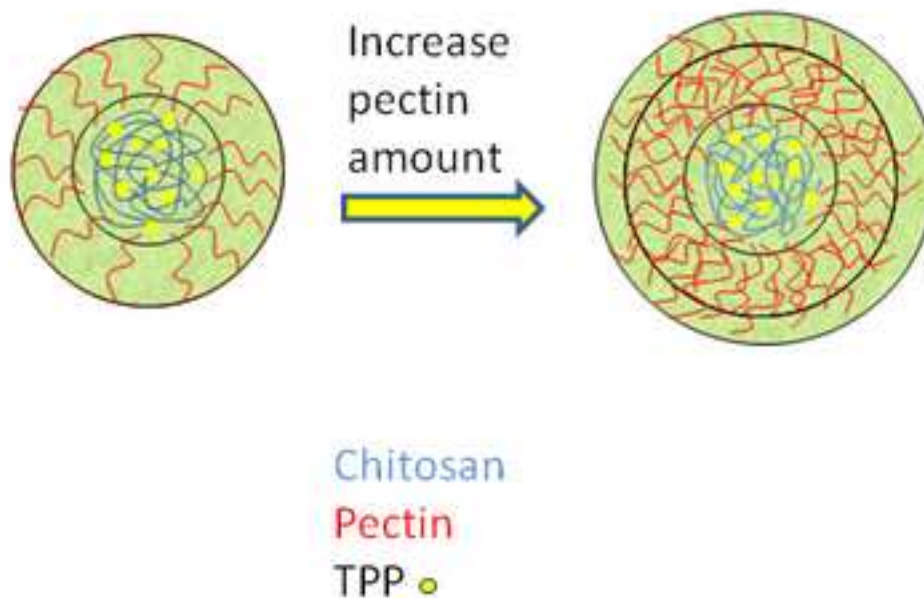
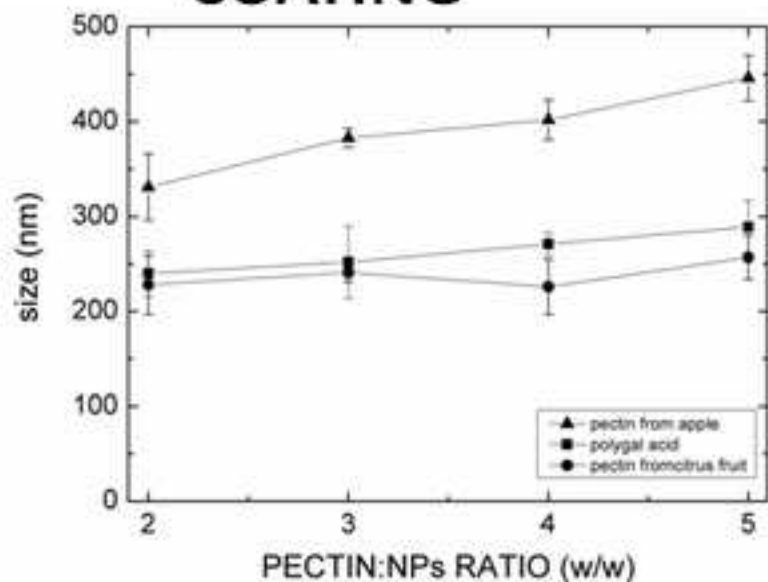
#### Rights / License:

The terms and conditions for the reuse of this version of the manuscript are specified in the publishing policy. For all terms of use and more information see the publisher's website.

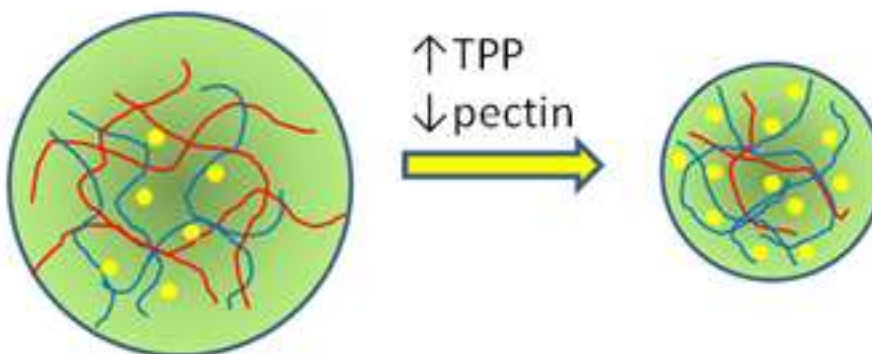
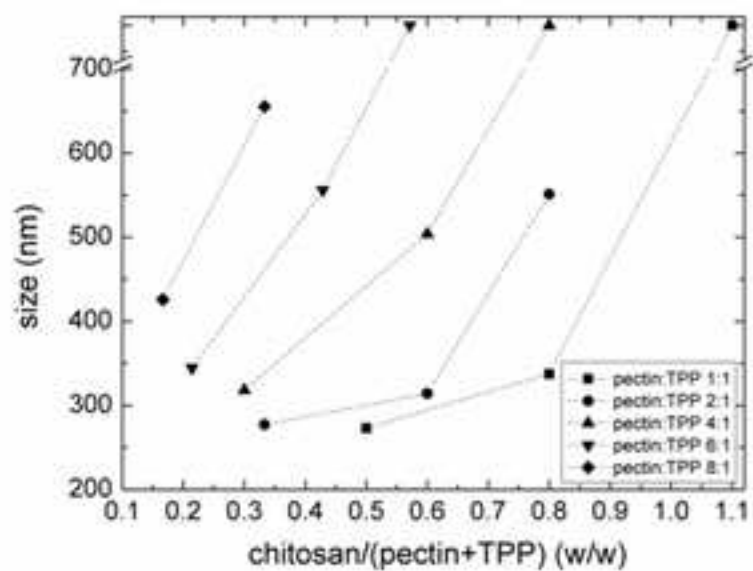
*This item was downloaded from IRIS Università di Bologna (<https://cris.unibo.it/>)*

***When citing, please refer to the published version.***

## COATING



## BLENDING



1 **Chitosan-pectin hybrid nanoparticles prepared by coating and blending techniques**

2  
3 Rampino A<sup>1§</sup>, Borgogna M<sup>1</sup>, Bellich B<sup>2,\*</sup>, Blasi P<sup>3,§,\*</sup>, Virgilio F<sup>1,4</sup>, Cesàro A<sup>2,4</sup>.

4  
5 Affiliations:

6 <sup>1</sup> Dept. of Life Sciences, University of Trieste, Via Giorgieri 5, 34127 Trieste, Italy

7 <sup>2</sup> Dept. of Chemical and Pharmaceutical Sciences, University of Trieste, Via Giorgieri 1, 34127  
8 Trieste, Italy

9 <sup>3</sup> Dept. of Chemistry and Technology of Drugs, University of Perugia, Via del Liceo 1,  
10 06123 Perugia, Italy

11 <sup>4</sup> Elettra-Sincrotrone Trieste, Strada Statale 14 km 163.5, Area Science Park, 34149 Trieste, Italy

12  
13  
14  
15 § Present addresses: A.R. Laboratorio Nazionale-Consorzio Interuniversitario Biotecnologie  
16 (LNCIB), Area Science Park, Padriciano 99, 34149 Trieste, Italy; P.B. School of Pharmacy, Via S.  
17 Agostino n.1, University of Camerino, 62032 Camerino (MC)

18  
19  
20  
21  
22  
23 \*Corresponding author: Barbara Bellich

24 e-mail address: bbellich@units.it

25 Tel.: +39 0405588742;

26 Fax.: +39 0405583903

27  
28 \*Corresponding author: Paolo Blasi

29 e-mail address: paolo.blasi@unicam.it

30 Tel.: +39 737402289;

31 Fax: +39 737637345

34 **ABSTRACT**

35

36 The preparation of chitosan nanoparticles in combination with pectins, as additional mucoadhesive  
37 biopolymers, was investigated. Pectin from apple and from citrus fruit were considered;  
38 polygalacturonic acid was taken as a reference. Tripolyphosphate was used as an anionic cross-  
39 linker. Two different techniques were compared, namely the coating and the blending. Coated  
40 nanoparticles (NPs) in the ratio pectin:NPs from 2:1 to 5:1 evidenced that the size of NPs increased  
41 as the amount of pectin (both from apple and citrus fruit) was increased. In particular, for NPs  
42 coated with pectin from citrus fruit the size ranges from 200 to 260 nm; while for NPs coated with  
43 pectin from apple the size ranges from 330 to 450 nm. A minimum value of Z-potential around -35  
44 mV was obtained for the ratio pectin:NPs 4:1, while further addition of pectin did not decrease the  
45 Z-potential. Also blended NPs showed a dependence of the size on the ratio of the components: for  
46 a given ratio pectin:tripolyphosphate the size increases as the fraction of chitosan increases; for a  
47 low ratio chitosan:pectin a high amount of tripolyphosphate was needed to obtain a compact  
48 structure. The effect of the additional presence of loaded proteins in chitosan-pectin nanoparticles  
49 was also investigated, since proteins contribute to alter the electrostatic interactions among charged  
50 species. FT-IR and DSC characterization are presented to confirm the interactions between  
51 biopolymers. Finally, the biocompatibility of the used materials was assessed by the chorioallantoic  
52 membrane assay, confirming the safety of the materials.

53

54

55 **Keywords:** Chitosan; pectin; hybrid nanoparticles; ionotropic gelation; coating and blending  
56 technique.

57

58

## 59 1. INTRODUCTION

60 Microspheres and microcapsules based on chitosan were developed for pharmaceutical applications  
61 and the importance of mucoadhesive properties for site specific drug delivery were described (He et  
62 al., 1998). The great potentiality of the use of chitosan as drug carrier is amply recognized. Various  
63 techniques have been described in literature for the preparation of chitosan microcarriers, as well as  
64 the parameters affecting drug release (Sinha et al., 2004). Different forms of chitosan based  
65 nanomaterials have been also reported in recent reviews (Borgogna et al., 2011; Shukla et al.,  
66 2012). The nanotechnological approach for the development of nanoparticle-based drug delivery  
67 systems has gained increase attention in the recent years (Desai, 2012). Several examples are  
68 reported in literature on the use of chitosan nanoparticles. More recently, rivastigmine loaded  
69 chitosan nanoparticles were investigated for intranasal delivery in case of Alzheimer's disease  
70 (Fazil et al., 2012); verapamil HCl loaded chitosan microspheres were studied for intranasal  
71 administration (Abdel Mouez et al., 2014); gemcitabine loaded in chitosan NPs was studied for oral  
72 delivery by Derakhshandeh and Fathi (2012).

73 One of the widely used techniques for the preparation of chitosan nanoparticles (NPs) is the ionic  
74 gelation, which is relatively simple and mild; it allows the successful encapsulation of labile  
75 molecules, such as proteins, since it avoids the use of organic solvents and high temperatures (Al-  
76 Qadi et al., 2012; Berger et al., 2004; Nasti et al., 2009; Xu and Du, 2003). The preparation of  
77 chitosan NPs following the method described by Calvo et al. (1997), was recently investigated  
78 focusing the attention on the effect of the ratio between chitosan and TPP (tripolyphosphate) on the  
79 loading of protein, being all charged species (Rampino et al., 2013). This study and other literature  
80 results (Papadimitiou et al., 2008; Bagre et al., 2013) show that small nanoparticles are obtained  
81 with a ratio of chitosan to TPP of 5:1. Moreover, chitosan is widely used for the preparation of  
82 several carriers due to its bioadhesive properties, its film forming abilities and low toxicity as well  
83 as its abundance in nature. Chitosan can interact with the constituents of the mucosal glycoprotein  
84 layer thus prolonging the residence time at the absorption site, increasing drug bioavailability  
85 (Sogias et al., 2012). The basic mechanisms of mucoadhesion have been reported and extensively  
86 commented (Andrews et al., 2009; Serra et al., 2009).

87 Pectin is another natural polysaccharide of pharmaceutical interest, whose properties mainly depend  
88 on the esterification degree. Its increasing use in the pharmaceutical field is due to its high  
89 availability in nature, its low or non toxicity nature and above all its mucoadhesive properties  
90 together with resistance to degradation by proteases and amylases. Such features make pectin  
91 attractive for the formulation of drug delivery carriers for many administration routes (Marras-

92 Marquez et al., 2015). In particular, the correlation between the mucoadhesive properties and the  
93 degree of methoxylation of different types of pectin has been investigated by Hagesaether et al.  
94 (2008). The same authors paid attention also to investigate the effect of formulation, i.e., when  
95 specific ions are added to the pectin solution. Indeed, on one side cross-linking can reduce the  
96 polymer mobility, therefore hampering its diffusion and interpenetration within mucin molecules;  
97 on the other side, particles of very small sizes have better potential to penetrate the mucus layer. In  
98 general, optimal size characteristics are required in order to achieve mucoadhesion by mean of the  
99 increased residence time and closer contact with mucosa. The possibility of obtaining hybrid  
100 nanoparticles, containing not only chitosan and TPP, but also other poly- or oligo-saccharides has  
101 been described in literature. Such hybrid systems are characterized by improved physical properties  
102 and better performances when used as drug delivery carriers (Goycoolea et al., 2009 and references  
103 therein).

104 The aim of this work was the investigation of two techniques, named coating and blending, for the  
105 preparation of hybrid pectin-chitosan nanoparticles.

106 Characterization of PEC properties in terms of size, charge, and surface morphology, shows the  
107 strict dependence on the macromolecular parameters of the polyions used (in addition to  
108 concentration, ionic strength, pH) and on the operative mixing conditions (interaction under resting  
109 or streaming mixing). For linear polymers the charge density (number of charges per unit length)  
110 defines not only the value for counterion condensation, but also the conditions for chain pairing.  
111 These comments may help the understanding of pectin-chitosan interaction with the co-presence of  
112 TPP, under the hypothesis of thermodynamic equilibrium. The practical effects of addition of pectin  
113 are investigated following the coating technique (post-synthesis of NPs) or the blending technique  
114 (during synthesis of NPs).

115 On one side the coating technique allows to create a core consisting of a polymer and a protein, thus  
116 ideally the protein is more protected from the outside environment due to the presence of an outer  
117 shell obtained by subsequent coating with a polymer. This is not presumably obtained by a blending  
118 technique where the protein is dispersed throughout the polymeric matrix. On the other side one of  
119 the main advantages of the blending technique is the possibility of the one-step formulation, that is  
120 not possible with the coating technique.

121 Thus, it has been possible to exploit the well known capability of chitosan to form nanoparticles, to  
122 obtain a drug delivery system based on the combination of two classes of mucoadhesive  
123 biopolymers.

## 124 **2. MATERIALS AND METHODS**

125

### 126 **2.1 MATERIALS**

127 Low molecular weight (LMW) chitosan (MW 150 kDa;  $[\eta] = 2.37$  dL/g; degree of acetylation DA  
128 = 13%), polygalacturonic acid from orange, MW 18 kDa, degree of esterification (DE) 10,6%  
129 (Cesàro et al., 1982), pectin from citrus fruit (MW 17 kDa, DE 22%), pectin from apple (MW 30-  
130 100 kDa, degree of esterification 71%), bovine serum albumin (BSA), albumin from chicken egg  
131 albumen (OVA), technical grade pentasodium tripolyphosphate (TPP), sodium acetate, sodium  
132 hydroxide, and sodium chloride were all purchased from Sigma-Aldrich Co. (St. Louis, Missouri,  
133 USA). Acetic acid and hydrochloric acid were obtained from Carlo Erba Reagents (Carlo Erba,  
134 Milan, Italy). All other chemicals were of the highest purity grade commercially available and used  
135 without further purification.

136 The commercial chitosan sample was purified and characterized as reported elsewhere (Donati et  
137 al., 2005). The intrinsic viscosity of chitosan was measured by employing a Schott-Geräte AVS/G  
138 automatic apparatus and an Ubbelohde type viscometer (in acetate buffer 0.25 M, pH 4.7), as  
139 reported in the previous paper (Rampino et al., 2013).

140

### 141 **2.2 METHODS**

#### 142 **2.2.1 Nanoparticles preparation**

143 Chitosan nanoparticles (NPs) were prepared using the ionotropic gelation method (Calvo et al.,  
144 1997; Rampino et al., 2013). A 0.25% w/v chitosan solution was prepared by dissolving LMW  
145 chitosan in 0.05% v/v acetic acid solution for 24 hours under stirring. The pH of the solution was  
146 adjusted to 5.5 with a sodium hydroxide solution while deionized water was added to obtain the  
147 desired final concentration. TPP was dissolved in deionized water at a concentration of 0.25% (w/v)  
148 and subsequently diluted to obtain solutions at different concentrations.

149 The TPP and chitosan solutions were filtered through a 0.45  $\mu\text{m}$  mixed cellulose esters membrane  
150 (Millipore, Massachusetts, USA) to remove any insoluble matter. TPP solution was added drop  
151 wise to the chitosan solution under magnetic stirring at room temperature (Rampino et al., 2013).

152 Chitosan NPs have been loaded with two different model proteins: BSA and OVA, whose  
153 isoelectric points are 4.8 and 4.7, respectively. The protein were dissolved in deionized water  
154 (concentration 4 mg/mL) and added directly to the chitosan solution under magnetic stirring.  
155 Batches with different theoretical loading were prepared by adding different volumes of the protein  
156 stock solution, to obtain final protein concentrations of 200, 400, and 600  $\mu\text{g/mL}$ . The solution,



157 containing chitosan and protein, was then diluted to a final volume of 5 mL using deionized water.  
158 After dropping the TPP solution, the dispersion was left under constant stirring for 30 min at room  
159 temperature. The suspension was centrifuged for 2 hours at 3270 RCF to remove the excess of  
160 chitosan and protein. The supernatant was collected separately while the sedimented particles were  
161 re-dispersed in deionized water, analyzed for their size and surface charge and then lyophilized.

162

### 163 **2.2.2 Pectin-chitosan nanoparticles**

164 Each pectin sample was dissolved in deionized water adjusting the pH between 6 and 7, thus  
165 forming the sodium salt. Hybrid pectin-chitosan NPs were prepared following two different  
166 procedures named coating (Borges et al., 2005) and blending (Alonso et al., 2006).

#### 167 ***Coating***

168 LMW Chitosan NPs suspension was added to a pectin solution drop wise at different ratios under  
169 magnetic stirring at room temperature. The suspension of coated particles was centrifuged for 2 h at  
170 3270 RCF and the supernatant was discarded. Particles were re-dispersed in deionized water,  
171 characterized and freeze dried. Protein loaded NPs were prepared according to the procedure  
172 reported for sole chitosan NPs (Rampino et al., 2013). Pectin-coated NPs were prepared by using  
173 sodium polygalacturonate, pectin from citrus fruit and pectin from apple.

#### 174 ***Blending***

175 Chitosan and TPP solutions were prepared as previously described. TPP solution was mixed under  
176 magnetic stirring to pectin solution at different volume ratios. NPs formed spontaneously upon drop  
177 wise addition of the cationic solution to the anionic one under stirring. NPs were isolated by  
178 centrifuging at 3270 RCF for 2 h, the supernatant was discarded and the pellet re-dispersed in  
179 deionized water, characterized and freeze dried. Loaded NPs were prepared dissolving the model  
180 protein directly in the anionic solution containing TPP and pectin, and then the particles were  
181 prepared as previously described. Blended NPs were prepared by using pectin from apple.

182

### 183 **2.2.3 Nanoparticle characterization: size and zeta potential**

184 The size of the NPs and the surface zeta potential were determined using a Malvern Zetasizer Nano  
185 ZS (Malvern Instruments, Worcestershire, UK). Measurements were carried out at 25 °C in  
186 replicate of three.

187

188

189

#### 190 **2.2.4 Determination of protein loading efficiency**

191 Six BSA and OVA standard solutions at different concentrations were prepared using a known  
192 amount of protein and analyzed with a bicinchoninic acid protein assay kit (BCA<sup>TM</sup>) Sigma-Aldrich  
193 Co. (St. Louis, Missouri, USA) to build a calibration curve. 25  $\mu\text{L}$  of each standard and sample  
194 were placed into a 96-well microplate and 200  $\mu\text{L}$  of reagent was added. Each analysis was  
195 performed in a replicate of three. The microplate was incubated at 37 °C for 30 minutes after being  
196 thoroughly mixed for 30 seconds by a microplate shaker. The microplate was then cooled to room  
197 temperature, and the absorbance measured on a plate reader (Pierce, Illinois, USA).  
198 Spectrophotometric measurements were carried out at 562 nm, which does not overlap with  
199 polymer spectra. Unloaded NPs were used as control.

200 The amount of protein loaded in NPs was calculated as the difference between the protein total  
201 amount and the protein recovered in the supernatant after centrifugation, assuming that the amount  
202 not found in the supernatant was encapsulated in the NPs.

203 The loading efficiency experiments were carried out on native NPs containing chitosan:TPP 5:1  
204 w/w, NPs coated with pectin from apple in the ratio from 2:1 to 5:1, loaded with BSA. Pectin from  
205 apple was used in blended NPs with a pectin:TPP ratio 4:1 w/w and a ratio between chitosan and  
206 the anionic components (pectin, TPP and protein) of 1.2:1 and 2:1, loaded with OVA.

207

#### 208 **2.2.5 Fourier transform-infrared (FT-IR) spectroscopy**

209 IR spectra were recorded on lyophilized samples using a Vertex 70 (Bruker Optics GmbH)  
210 spectrophotometer (spectral resolution of 4  $\text{cm}^{-1}$ ) equipped with a MIRacle<sup>TM</sup> ATR devices (Pike  
211 Optics) with a single reflection diamond crystal (1.8 mm spot size) and using a MCT detector  
212 (HgCdTe, mercury-cadmium-tellurium) cooled with liquid nitrogen.

213 Samples of the raw materials and freeze dried NPs were placed on the top of the diamond crystal  
214 and stopped with a high-pressure clamp. Spectra were recorded in the range 5000-600  $\text{cm}^{-1}$ .

215 FT-IR investigations were carried out on starting materials, chitosan:TPP NPs, coated NPs with  
216 pectin from apple and citrus fruit, blended NPs with pectin from apple.

217

#### 218 **2.2.6 Differential Scanning Calorimetry (DSC)**

219 DSC analysis of raw materials, freeze dried uncoated, coated and blended pectin-chitosan NPs was  
220 carried out by using a PerkinElmer<sup>®</sup> DSC 6 calorimeter (PerkinElmer, Massachusetts, USA).  
221 Samples (about 2 mg) were accurately weighed into open aluminum pan and heated from 20 °C to  
222 350 °C at a scanning rate of 10 °C/min under a nitrogen flow of 20 mL/min.

223 DSC investigations were carried out on on starting materials, chitosan:TPP NPs, coated NPs with  
224 pectin from apple and citrus fruit, blended NPs with pectin from apple.

### 225 **2.2.7 Chorioallantoic membrane assay**

226 The safety of raw materials (chitosan and pectin from apple), chitosan NPs and chitosan NPs coated  
227 with pectin from apple in the ratio pectin:NPs 2:1 w/w was evaluated *in vivo* by using the chick  
228 embryo chorioallantoic membrane (CAM) assay (Saw et al., 2008; Schoubben et al., 2013).  
229 Fertilized eggs were disinfected with alcohol 70° and placed in an incubator at 38 °C with 60%  
230 relative humidity. At incubation day 3, a window opening was punctured at the blunt end of the egg  
231 and living embryos were selected for the experiment. The opening was then covered with a  
232 polyethylene film glued with albumen to avoid water loss and microbial contamination. At  
233 incubation day 6, solid samples (6 mm tablet) were applied directly on the CAM. A Leica WILD  
234 M32 stereomicroscope (equipped with a WILD PLAN 1X lens), connected to a Leica DFC 320  
235 camera system, was used to follow the evolution of any effect on the materials on the CAM. After  
236 24 hours, all the eggs were examined again and all the acquired images were compared with those  
237 at time 0 and with the controls for qualitative acute toxicity evolution (Vargas et al., 2007).

238

## 239 **3. RESULTS AND DISCUSSION**

240

### 241 **3.1. Chitosan and pectin samples used in nanoparticle preparation.**

242 LMW chitosan NPs, produced following a previous optimized methodology, had a mean size and  
243 surface charge of  $200 \pm 24$  nm and  $25 \pm 3$  mV, respectively (Rampino et al., 2013). The production  
244 of hybrid pectin-chitosan NPs as drug delivery systems was investigated in view of the well-known  
245 mucoadhesive properties of pectins. The pectin samples were characterized by different values of  
246 molecular weight and degree of esterification (MW and DE, respectively): polygalacturonic acid  
247 (18 kDa and 10.6%), pectin from citrus fruit (17 kDa and 22%), pectin from apple (30-100 kDa and  
248 71%). These macromolecular properties of the pectins and of chitosan sample used (MW 140 kDa  
249 and DE 13%) in addition to the coating or blending procedure used, govern and control the final  
250 characteristics of the hybrid NPs that can be effectively defined as poly-electrolyte complexes  
251 (PEC).

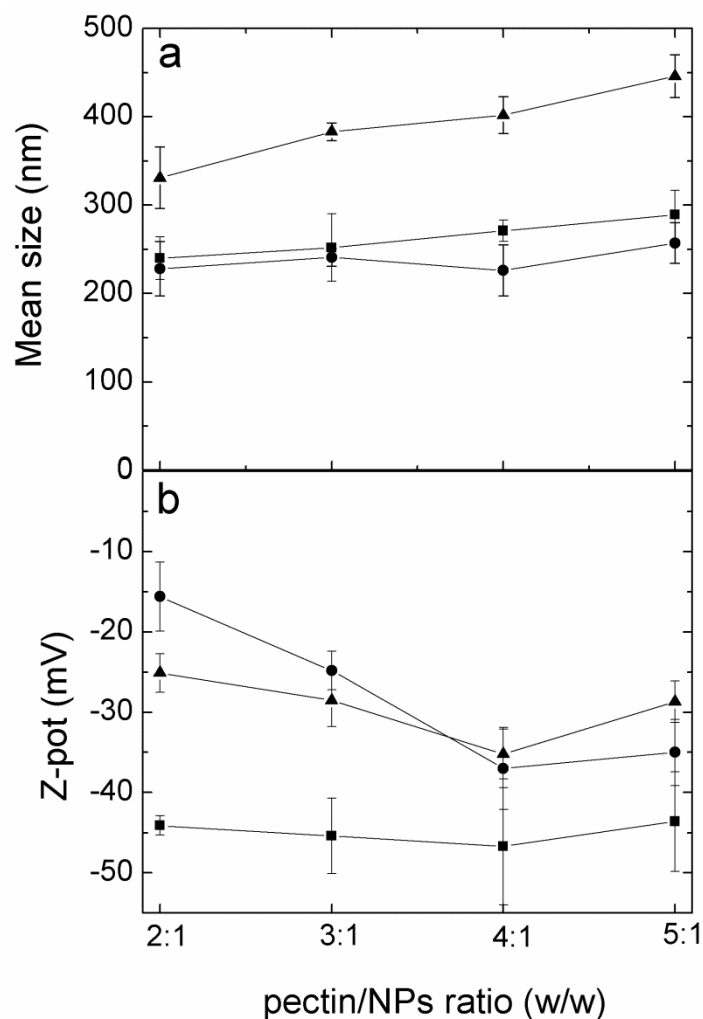
252

### 253 **3.2. Pectin-chitosan nanoparticle preparation and characterization**

#### 254 **3.2.1. Coating technique**

255 Chitosan NPs, obtained using a chitosan:TPP ratio of 5:1 w/w, were centrifuged, re-dispersed and  
256 added to the pectin solution. Since chitosan NPs are characterized by a net positive surface charge  
257 and pectin is negatively charged at the pH (6-7) employed for the coating, the electrostatic  
258 interaction between opposite charges favors the complexation of pectin on the NPs outer surface.  
259 This is seen by the dependence of NPs size and Z-potential on the degree of esterification,  
260 molecular weight and concentration of the pectin used, as reported in **Fig. 1**.

261



262

263 **Fig. 1:** mean size (a) and Z-potential (b) of chitosan NPs (chitosan:TPP ratio 5:1 w/w) coated with  
 264 sodium polygalacturonate (■), pectin from citrus fruit (●) and pectin from apple (▲).

265

266 In all cases, an increase of the mean size is observed and, supposing that pectin is confined in the  
 267 outer layer (coating), the thickness of the coating depended on the type and amount of pectin used.  
 268 A remarkable size increase was recorded when apple pectin was used to coat chitosan NPs (**Fig.**  
 269 **1a**), while a smaller increase in NPs size is produced with sodium polygalacturonate or citrus  
 270 pectin. The behavior of apple pectin coating is clearly due to its higher MW and higher DE as  
 271 compared with the other two pectin samples that show similar behavior due to the quite similar  
 272 values of molecular weight and charge density of the two macromolecules.

273 As a further general comment, the larger the amount of pectin, the higher was the increase in  
 274 particle size. However, this effect is particularly evident for the apple pectin, since the presence of a  
 275 higher amount of low-charged polymer increases the coating thickness. As a speculative

276 observation (to be confirmed with the other results here reported), a more swollen coating would  
277 occur with apple pectin that has the highest DE.

278 As the pectin concentration is concerned, at pectin:NPs ratio less than 2:1, both apple and citrus  
279 pectins led to the formation of aggregates (data not shown), probably because of the low surface  
280 charge. Indeed, upon increasing pectin concentration the surface charge of NPs changes from  
281 positive to slightly negative producing particles with a Z-potential of -6 mV (data not shown), while  
282 for NPs stability a high charged surface is required to avoid their aggregation. It has been shown  
283 that such a low absolute value of Z-potential does not produce an efficient electrostatic repulsion  
284 between NPs leading to aggregation (Gonzalez-Mira et al., 2010).

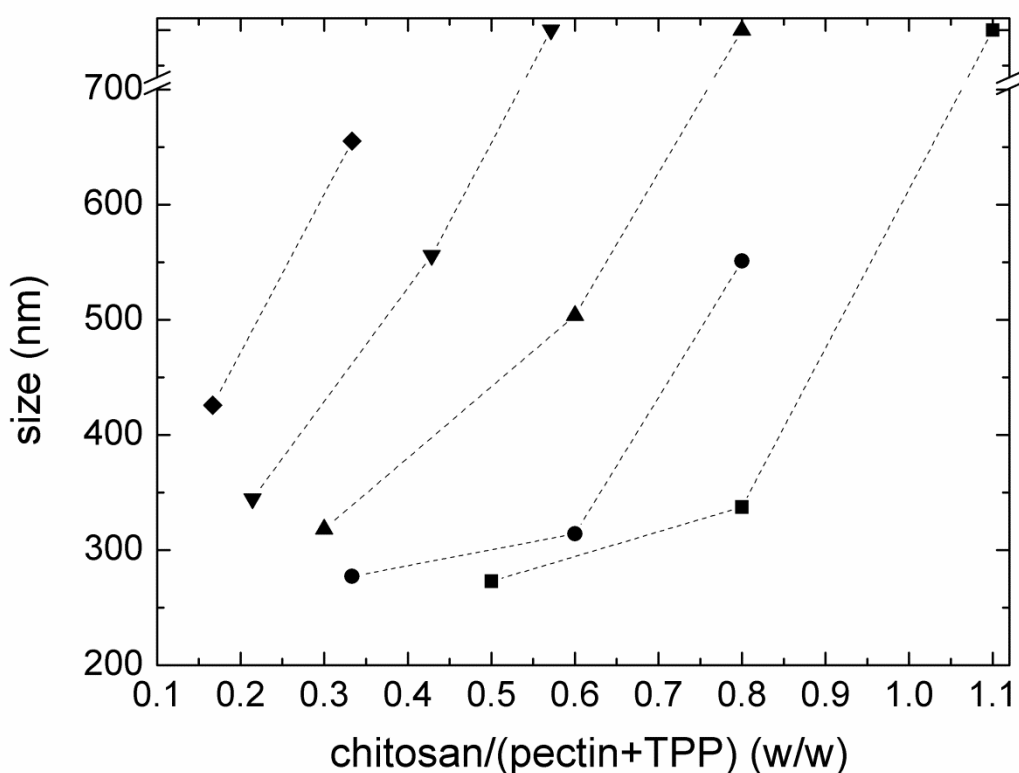
285 **Fig. 1b** reports the NPs surface charge as a function of the pectin:NP ratio. At low pectin  
286 concentration (2:1) the value of Z-potential is very negative for sodium polygalacturonate (*ca* -45  
287 mV), while for citrus pectin and for apple pectin is about -25 and -15 mV, respectively. Upon  
288 increasing pectin concentration, no changes in Z-potential are observed with sodium  
289 polygalacturonate, while both apple and citrus pectins reached a minimum value of about -35 mV at  
290 pectin:NPs ratio of 4:1 (**Fig. 1b**). These findings suggest that an optimal level of coating (as derived  
291 from the value of Z-potential due to polymers complexation) can be identified and that a further  
292 addition of pectin to NPs only produces an increase in size.

293

### 294 **3.2.2. Blending technique**

295 The preparation of NPs by blending technique implies that chitosan is added to the anionic solution  
296 of pectin containing TPP, with the important advantage of a one-step procedure. The effect of the  
297 amount of pectin on NPs size has been investigated both as a function of the mass ratio between the  
298 cationic (chitosan) and anionic (pectin+TPP) components, and as a function of the ratio between  
299 pectin and TPP (**Fig. 2**).

300 For a given ratio between pectin and TPP, it was generally observed a size increase as the mass  
301 fraction of chitosan increased. A remarkable size increase was observed when a high amount of  
302 pectin was used and the ratio between pectin and TPP was high. A concomitant reduction of  
303 chitosan and pectin and an increase of TPP amount provoked a reduction of particle size. This  
304 might be due to the strong effect of TPP that produced a compact structure with chitosan that  
305 interacts with pectin. Thus, the dependence of the complexation stoichiometry on the reaction of the  
306  $[-\text{COO}^-]$  and  $[-\text{NH}_3^+]$  functional groups of both polyelectrolytes was established, expressed as the  
307 ratio of the chitosan concentration in the NPs relative to the total pectin concentration.



309

310 **Fig. 2:** mean size of chitosan NPs blended with apple pectin in different ratios with TPP. Ratio  
 311 pectin:TPP 1:1 (■), 2:1 (●), 4:1 (▲), 6:1 (▼) and 8:1 (◆). The mean size of NPs in the absence of  
 312 pectin is in the range of 200 nm.

313

314 For the same chitosan mass fraction, NPs with different size can be obtained depending on the ratio  
 315 between pectin and TPP. A low mean size of NPs was obtained for formulations with a low  
 316 pectin:TPP ratio. This is not surprising since a high concentration of TPP, available for ionic  
 317 complexation, produces a highly compact polyelectrolytes network. When the concentration of  
 318 pectin increased, the electrostatic interactions with less accessible  $\text{-NH}_3^+$  groups resulted in the  
 319 formation of more swollen structures; this is due to the increase in the promotion of un-complexed  
 320 stretches of the pectin chains. A trend for NPs size can be recognized suggesting that the lowest size  
 321 of NPs (less than 300 nm) is obtained for chitosan mass fractions in the range between 0.3 and 0.5,  
 322 and with pectin:TPP ratio 1:1 to 4:1.

323 A general decrease of the Z-potential was found as the amount of pectin was increased reaching  
 324 values between -20 and -29 mV. For the same fraction of chitosan, NPs with different surface  
 325 charge can be obtained depending on the ratio between pectin and TPP. For a given ratio, the lowest

326 surface charge is obtained with the highest ratio pectin to TPP. This aspect is particularly important  
327 in view of modulating NP surface properties.

328 As mentioned, the blending technique is preferred from the operational point of view since tedious  
329 steps, such as centrifugation and re-dispersion, are not necessary. In addition, the blending  
330 technique resulted suitable to prepare NPs even at chitosan:TPP ratio lower than 5:1 w/w, while this  
331 was not possible using the coating technique because of aggregation.

332

### 333 **3.3 Effect of protein loading**

334 The effect of two model proteins, BSA and OVA, was investigated since the addition of proteins to  
335 the formulation, either blending or coating, can further modify the equilibria established among  
336 chitosan, pectin and TPP, in relation to the charged groups on the protein surface (Yu et al., 2009).  
337 OVA and BSA are medium size globular protein with a molar mass of 45 and 66.5 kDa,  
338 respectively, a similar isoelectric point (4.9 and 4.7) and equal absolute negative charge of about -  
339  $11e$  at pH 7. Therefore, the only difference would reside in the dimensions, being OVA 2/3 smaller  
340 than BSA (Stokes radius 3.1 and 3.5, respectively).

341 The loading efficiency of experiments were carried out on native NPs containing chitosan:TPP 5:1  
342 w/w and NPs coated with pectin from apple in the ratio from 2:1 to 5:1. With the coating technique,  
343 the loading efficiency for BSA was similar to that found for uncoated NPs (chitosan:TPP 5:1 w/w),  
344 and ranging between 40% and 60% (Rampino et al. 2013), suggesting that the final step of coating  
345 did not induce protein loss. Furthermore, while the presence of protein did not significantly increase  
346 the size of the NPs, however, a relevant increase of the dimensions was detected after the coating  
347 with pectin. A direct correlation was found with the amount of pectin added, loaded NP mean  
348 diameter ranging from 700 nm to 1250 nm for ratio of pectin to NPs from 2:1 to 5:1 w/w. Given the  
349 pI of OVA and BSA (both slightly negative charged), an electrostatic interaction occurs between  
350 the positively charged chitosan and the negatively charged proteins, therefore screening chitosan for  
351 further interaction with pectin and producing much less compact polymer particles. Loaded NPs  
352 were characterized by Z-potential values slightly lower than unloaded NPs. In addition, the decrease  
353 of the Z-potential was as pronounced as the loading increased. The subsequent addition of pectin  
354 completely changes the surface charge from positive to negative. The Z-potential was around -38  
355 mV, sufficient to maintain a permanent electrostatic repulsion and avoid the aggregation.

356 Pectin from apple was used in blended NPs with a pectin:TPP ratio 4:1 w/w and a ratio between  
357 chitosan and the anionic components (pectin, TPP and protein) of 1.2:1 and 2:1. Regarding the



358 blending technique, experiments with OVA suggested a possible competition between pectin and  
359 ovalbumin. Indeed, the loading efficiency, ranging between 16% and 27%, was lower than the  
360 corresponding unblended; pure chitosan NPs had a loading efficiency between 48% and 76%  
361 (Rampino et al. 2013), depending on the initial amount. A decrease of the loading efficiency was  
362 found as the amount of pectin increased and minor effects were observed on NPs size (an increase  
363 of about 50 nm was observed), while the value of Z-potential was similar to that of unblended NPs.

364

### 365 **3.4 FTIR-ATR spectroscopic evidence for polymer interaction**

366 FT-IR investigations were carried out coated NPs with pectin from apple and citrus fruit and  
367 blended NPs with pectin from apple; for comparison starting materials and native chitosan:TPP NPs  
368 are also reported. The solid state studies (FT-IR and DSC) have been conducted on empty NPs. The  
369 presence of a protein would have added another variable for the experiments. Chitosan spectrum  
370 shows a broad absorption between 3350 and 3270  $\text{cm}^{-1}$  (**Fig. 3a**) previously attributed to a  
371 combination of stretching modes of O-H and N-H bonds in chitosan and to hydrogen bonds among  
372 polysaccharide chains. **Fig. 3a** shows that the same band becomes broader and shifted to lower  
373 wavenumbers in the sample of chitosan NPs, thus indicating an enhancement of the hydrogen bonds  
374 system (Mishra et al., 2008). The main peaks recognized for the chitosan sample were related to  
375 C=O stretching amide I at 1635  $\text{cm}^{-1}$  and to amide II at 1539  $\text{cm}^{-1}$  (Woranuch and Yoksan, 2013).  
376 These peaks slightly shifted to 1633  $\text{cm}^{-1}$  and to 1543  $\text{cm}^{-1}$  in the chitosan NPs sample, with an  
377 increase of intensity for the latter. The presence of this intense band at 1543  $\text{cm}^{-1}$  is attributed to the  
378 bond formation between the amino groups of chitosan and TPP (Azevedo et al., 2011). Similar  
379 considerations were done by Xu and Du (2003) studying chitosan film treated with  $\text{NaH}_2\text{PO}_4$   
380 (Knaul et al., 1999). Other characteristic bands of chitosan NPs are the peak at 1213  $\text{cm}^{-1}$  attributed  
381 to the P=O of the TPP, the intense band around 1070  $\text{cm}^{-1}$  corresponding to C-O stretching and the  
382 pyranose ring at 890  $\text{cm}^{-1}$  (Woranuch and Yoksan, 2013).

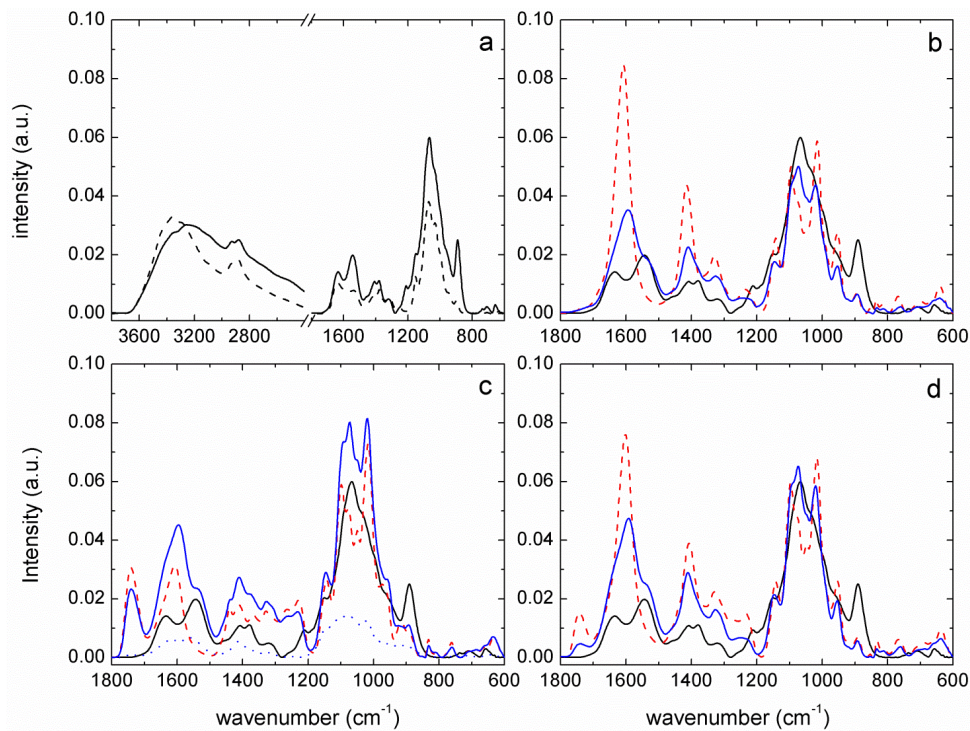
383 **Fig. 3b-d** reports the FTIR spectra of chitosan NPs coated with the three different pectin considered  
384 (sodium polygalacturonate, apple pectin and citrus fruit pectin) or blended with apple pectin. The  
385 spectra are reported in the range between 600  $\text{cm}^{-1}$  and 1800  $\text{cm}^{-1}$ , since major changes occur within  
386 this range. The region 1000 – 1200  $\text{cm}^{-1}$  contains skeletal C-O and C-C vibration bands of  
387 glycosidic bonds and pyranose ring (Synytsya et al., 2003).

388 The main changes were in the region 1500-1700  $\text{cm}^{-1}$  corresponding to the stretching vibrations of  
389 amide bond and indeed the interaction of chitosan with pectin involves amine groups on chitosan  
390 (not yet involved in bonds with TPP) and carboxylic groups of pectin (**Fig. 3b**).

391 Polygalacturonate shows only one peak around 1608  $\text{cm}^{-1}$ ; the two characteristic peaks of chitosan  
392 NPs disappeared giving only one peak at 1593  $\text{cm}^{-1}$  with a small shoulder after the coating with  
393 polygalacturonate. A peak at 1410  $\text{cm}^{-1}$  was identified and attributed to C-OH stretching of the  
394 carboxylic group (Synytsya et al., 2003), as similarly observed for alginate (Sarmiento et al., 2006a).

395 Apple pectin and citrus fruit pectin (**Fig. 3c-3d**) are characterized by the C=O stretching at 1608  
396 and 1600  $\text{cm}^{-1}$  respectively and by an additional peak, respectively at 1741 and 1743  $\text{cm}^{-1}$ ,  
397 corresponding to the C=O stretching in the ester form (Synytsya et al., 2003). In the apple pectin  
398 sample the two peaks of C=O stretching have comparable intensity, due to the high degree of  
399 esterification. As similarly observed for the polygalacturonate, the coating with apple pectin and  
400 citrus fruit pectin gives rise to a single peak, respectively at 1597 and 1591  $\text{cm}^{-1}$ , due to the  
401 presence of the pectin on the surface on the NPs, and a small shoulder, in both cases at 1535  $\text{cm}^{-1}$ ,  
402 as already commented for the chitosan NPs formation. The peak around 1400  $\text{cm}^{-1}$ , that was a  
403 double peak in the chitosan NPs, becomes a single peak and it is shifted to 1410  $\text{cm}^{-1}$  after coating.

404 The peaks attributed to the stretching of C=O in the ester form are still visible, but less intense. The  
405 shifts observed in the two pectins vary only slightly from one to another, probably suggesting that  
406 the different degree of esterification does not affect the number of interactions that are formed with  
407 amino groups of chitosan.



408

409

410 **Fig. 3.** FTIR spectra of a) chitosan (dash line) and chitosan NPs (full line); b) chitosan NPs (black  
 411 full line), polygalacturonate (red dash line), polygalacturonate coated NPs (blue full line); c)  
 412 chitosan NPs (black full line), apple pectin (red dash line), apple pectin coated NPs (blue full line)  
 413 and apple pectin blended NPs (blue dot line); d) chitosan NPs (black full line), citrus fruit pectin  
 414 (red dash line), citrus fruit pectin coated NPs (blue full line).

415

416 The effect of the shift is more pronounced for the sample coated with polygalacturonate. The  
 417 important outcome is that the shift of these bands indicates a change in the environment of amino  
 418 and carboxyl groups through the mutual interaction (Bigucci et al., 2008). From the presence of  
 419 peaks different from those of the uncoated NPs it was possible to confirm the existence of a coating  
 420 layer of pectin around the NPs, as also commented for alginate (Borges et al., 2005).

421 **Fig. 3c** reports the spectra of pectin-chitosan NPs obtained by blending technique. It has to be  
 422 noticed that the bands are broader than that found for the corresponding coated NPs. A weak peak  
 423 at  $1741\text{ cm}^{-1}$  corresponding to the C=O stretching of the ester group of the pectin is still observed.  
 424 The peak at  $1608\text{ cm}^{-1}$  corresponding to the asymmetric stretching of carboxylate group shifts to  
 425  $1597\text{ cm}^{-1}$  in case of the coated NPs; in case of the blended NPs it is still possible to identify the  
 426 two peaks characterizing the chitosan NPs, at  $1635\text{ cm}^{-1}$  and  $1542\text{ cm}^{-1}$ , but these peaks are shifted  
 427 of a few  $\text{cm}^{-1}$  (to  $1616\text{ cm}^{-1}$  and to  $1564\text{ cm}^{-1}$ ) and are of comparable intensity.

428 The shift of the band at  $1564\text{ cm}^{-1}$  (attributed to N-H bending) is greater than what has been  
429 observed in the coated samples. This could be due to the fact that the bending modes are sensitive to  
430 the changes in the environment of the group and so are more affected by a perturbative surrounding  
431 than the stretching modes. Therefore this shift of the N-H bending band could be indicative of a  
432 greater number of interaction between the amino groups of chitosan and the carboxyl groups of  
433 pectin, compared to the coated samples (Bigucci et al., 2008).

434

### 435 **3.5 Differential scanning calorimetry**

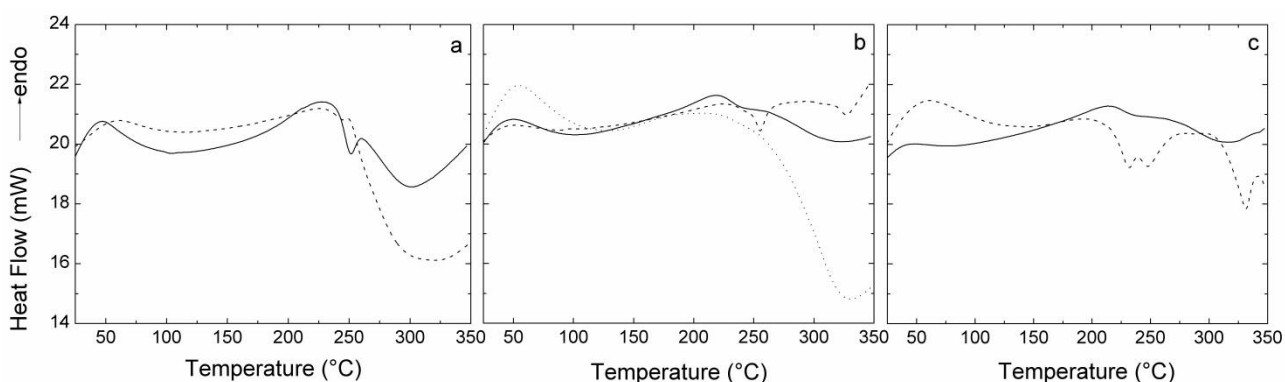
436 DSC investigations were carried out on coated NPs with pectin from apple and citrus fruit and on  
437 blended NPs with pectin from apple; for comparison starting materials and native chitosan:TPP NPs  
438 are also reported. DSC data of pure chitosan are characterised by an endothermic event (peak temp  
439 at  $57.2\text{ }^{\circ}\text{C}$ ) corresponding to the dehydration and by an exothermic event that begins at  $252\text{ }^{\circ}\text{C}$  with  
440 a peak around  $320\text{ }^{\circ}\text{C}$  corresponding to the thermal degradation (Sarmiento et al., 2006a; Sarmiento  
441 et al., 2006b). In addition to the dehydration endothermic event (peak at  $54.3\text{ }^{\circ}\text{C}$ ), chitosan NP DSC  
442 data revealed another endothermic event at  $225\text{ }^{\circ}\text{C}$  that has been ascribed to the breakdown of  
443 unspecific electrostatic interactions by Borges et al. (2005). The authors reported also a second  
444 endothermic peak of minor intensity, related to the cleavage of electrostatic interactions between  
445 chitosan and the counterion (sulphate ions in that case). In our case (TPP as counterion) a similar  
446 second peak was observed, and it is similarly attributed to the cleavage of such interactions. Indeed,  
447 the thermogram of TPP alone evidenced an endothermic peak at  $192\text{ }^{\circ}\text{C}$ ; therefore, it could also  
448 derive from the TPP, although shifted to higher temperatures in NPs. The exothermic event  
449 beginning at  $243.8\text{ }^{\circ}\text{C}$  with a peak around  $310\text{ }^{\circ}\text{C}$ , and corresponding to thermal degradation, is  
450 slightly shifted to lower temperatures (Bagre et al., 2013) as a result of the interaction of chitosan  
451 with TPP (Azevedo et al., 2011). The intensity of the exothermic event for chitosan NPs is lower  
452 than that of the native chitosan (similar weight are compared); this is reasonably due to the fact that  
453 a fraction of the chitosan chain is cross-linked with TPP and therefore differently susceptible to  
454 degradation.

455 Pectin from apple is characterized by the endothermic event corresponding to dehydration and by  
456 two sharp exothermic peaks at  $255\text{ }^{\circ}\text{C}$  and  $328\text{ }^{\circ}\text{C}$ , corresponding to degradation (**Fig. 4b**). Apart  
457 from the endothermic event of dehydration, chitosan NPs coated with apple pectin are characterized  
458 by an exothermic event starting at  $273\text{ }^{\circ}\text{C}$  with a peak at  $324\text{ }^{\circ}\text{C}$ , suggesting a thermal stabilization  
459 due to the interaction of chitosan with pectin and not only to TPP. The interaction is also confirmed

460 by the absence of any characteristic peaks of the pectin. The thermogram of pectin chitosan blended  
461 NPs did not reveal any characteristic peak of the apple pectin; the only difference observed was that  
462 the height of the exothermal event is far higher than that of the chitosan NPs and it is similar to  
463 chitosan alone, so not cross-linked with TPP. A lower interaction between chitosan and TPP,  
464 reasonably due to a competition between TPP and pectin, both negatively charged, would explain  
465 the recorded data.

466 Pectin from citrus fruit is characterized by an exothermal event between 225 and 250 °C with two  
467 distinct peaks at 232 and 248 °C, and another exothermal sharp peak at 331 °C (**Fig. 4c**). The  
468 thermogram of chitosan NPs coated with citrus fruit pectin is characterized by an exothermic event  
469 with a peak at 318 °C, similar to that of NPs coated with apple pectin. As previously commented for  
470 apple pectin samples, characteristic peaks of the citrus fruit pectin were not found, confirming the  
471 interaction of pectin with chitosan as already evidenced by surface charge measurements.

472



473

474

475 **Fig. 4:** DSC curves of a) chitosan (dash line) and chitosan NPs (straight line); b) apple pectin (dash  
476 line), coated NPs (straight line) with pectin and blended NPs (dot line) with pectin; c) citrus fruit  
477 pectin (dash line) and coated NPs (straight line) with pectin.

478

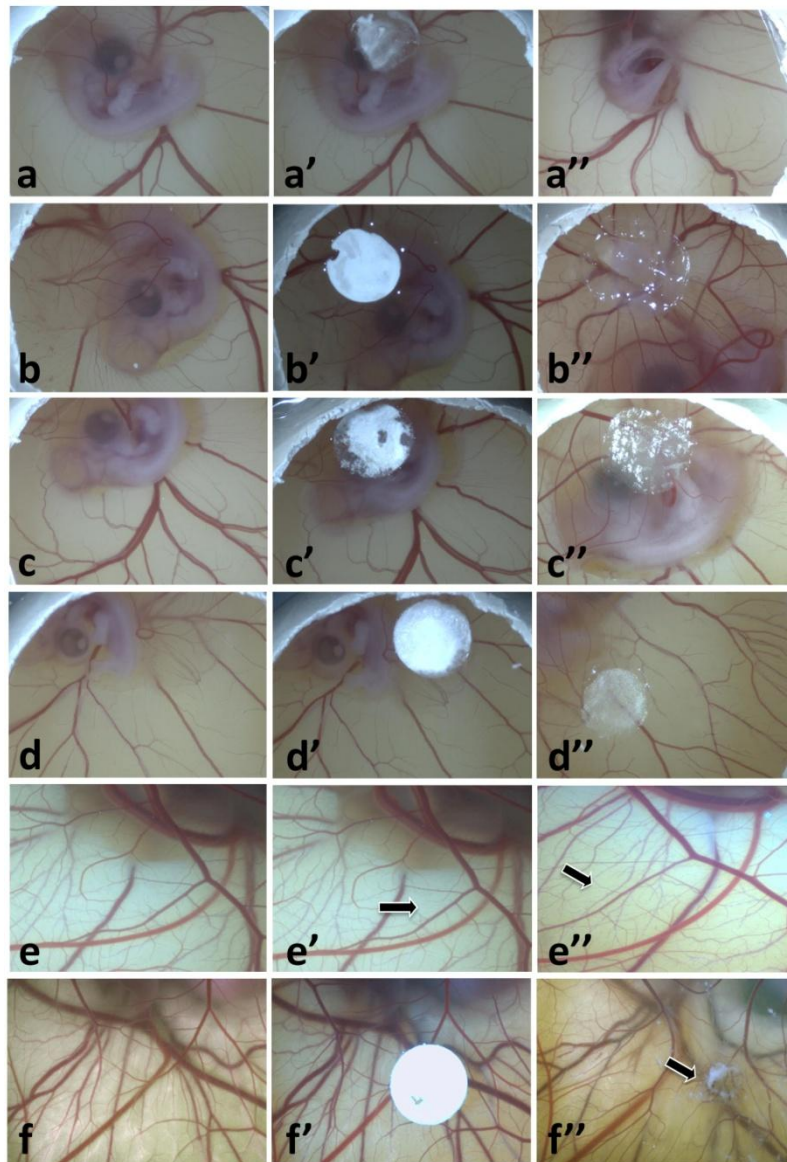
### 479 3.6 Chorioallontoic membrane assay (CAM)

480 CAM of 6 days old chicken embryos are shown in **Fig. 5a-d**. Because of eggs incubation in vertical  
481 position (convex pole in upper position), CAM floats over the yolk sack and, while growing, will  
482 cover all the air-exposed surface adhering to most of the testaceous membrane internal surface.  
483 Intrinsic CAM characteristics (e.g., high transparency, high vascularization and capillarity,  
484 sensitivity to physical and chemical insults) give this structure the right features for the direct and  
485 continuous evaluation of acute inflammatory response (Vargas et al., 2007; Saw et al., 2008).

486 The tested materials showed different behaviors in terms of dissolution/dispersion in the albumen  
487 wetting CAM surface. After deposition on CAM surface, pectin from apple swelled and  
488 polysaccharide chains rapidly disperse in the albumen film covering the membrane (**Fig. 5a' and**  
489 **5a''**). The material was not visible 24 hours after deposition. On the contrary, 24 hours after  
490 deposition, chitosan, chitosan NPs, and chitosan-pectin NPs swelled generating transparent gels that  
491 did not disperse in the albumen film (**Fig. 5**). Transparency allowed to visualize easily the portion  
492 of CAM under the material and not just the space around the implant. A careful observation of  
493 treated embryos (1 day after treatment) evidences the complete absence of the signs ascribable to  
494 acute toxicity, inflammation or pro-angiogenic effect, and no substantial differences were evidenced  
495 between the raw materials and NPs (**Fig. 5**). The same results are obtained with saline, the negative  
496 control routinely employed in our laboratories in this experimental setup (Blasi et al., 2013) and  
497 confirmed here (**Fig. 5**). TPP, being ionically bound to chitosan amino groups, does not impair the  
498 biocompatibility of the NPs evaluated. TPP has shown to be extremely toxic with the same  
499 experimental setup (Rampino et al., 2013). Membrane opacity, bleeding, vessel rupture, CAM  
500 corrosion, capillary and vessel overgrowth, are the classical reactions to substances or materials  
501 provoking a toxic insult or an inflammation on this extraembryonic membrane. Additionally, a  
502 substance having pro- or anti-angiogenic effect is responsible of the increase or decrease of  
503 capillaries/vessels density under and/or around the treated zone. These effects are experienced by  
504 depositing aggressive surfactants, such as sodium dodecylsulphate (Blasi et al., 2013), or  
505 polysaccharides, such as  $\lambda$  carrageenan (**Fig. 5**), that are used as positive controls.

506

507



508

509 **Fig. 5** Chicken embryos at different stages of development observed during acute toxicity  
 510 experiments. a, embryo before treatment; a', after material (apple pectin) deposition; a'' after 24  
 511 hours - b, embryo before treatment; b', after material (chitosan) deposition; b'' after 24 hours - c,  
 512 embryo before treatment; c', after material (chit/pect NPs) deposition; c'' after 24 hours - d, embryo  
 513 before treatment; d', after material (chit NPs) deposition; d'' after 24 hours - e, embryo before  
 514 treatment; e', after saline deposition (negative control); e'' after 24 hours - f, embryo before  
 515 treatment; f', after material ( $\lambda$  carrageenan) deposition (positive control); f'' after 24 hours.

516

517

518

519

520 **4. CONCLUSIONS**

521 Chitosan in combination with pectins confirmed to be a valuable biopolymer for the preparation of  
522 carriers interesting for drug delivery applications, due to the possibility to tailor the physico-  
523 chemical characteristics of the final NPs.

524 The most relevant outcome is the large number of potentially useful nanoparticles prepared with the  
525 two procedures, which, however, has been a challenge for selecting a few batches for  
526 characterization and testing studies. A rationalization would imply that the actual composition of  
527 NPs and not simply the starting composition is taken as a characterizing parameter of the products.  
528 Unfortunately, to the best of our knowledge, this approach is not yet reported in literature. The  
529 results here presented evidenced that it was possible to prepare pectin:chitosan NPs with both  
530 techniques, as already reported for other polymers. Two main advantages resulted from the  
531 blending technique: the first is the one-step preparation, that is highly desirable especially in view  
532 of a scale-up process, the second one is the possibility to tune the size and Z-potential by properly  
533 selecting the ratio of chitosan, pectin and TPP. The coating technique did not allow such a  
534 modulation of size, since the addition of pectin as external NPs coating always increases the size. It  
535 is worth noticing that the addition of a protein requires to take into account the competition among  
536 charged species. Indeed, a decrease of the loading of BSA and OVA was found in case of the  
537 blending technique due to the electrostatic interactions of chitosan with protein and pectin, both  
538 negatively charged. This brings to the conclusion that the most suitable technique depends on the  
539 physico-chemical characteristics of the species involved, i.e. polymer and protein.

540

541 **Acknowledgment**

542 This work has been partially carried out within the European Project FP6 NanoBioPharmaceutics  
543 (NMP 026723-2). Antonio Rampino was the recipient of a grant from MIUR (Rome) during his  
544 Ph.D. studies on “Polysaccharide-based nanoparticles for drug delivery”. The Authors are indebted  
545 to Mr. Lanfranco Barberini for the precious support in chicken embryo chorioallantoic membrane  
546 assay.

547

548

549

550

551

552



553

554

555 **References**

- 556 Alonso-Sande, M., Cuña, M., Remuñán-López, C., Teijeiro-Osorio, D., Alonso-Lebrero, J.L.,  
557 Alonso, M.J., 2006. Formation of new glucomannan-chitosan NPs and study of their ability to  
558 associate and deliver proteins. *Macromolecules*, 39, 4152-4158.
- 559 Al-Qadi, S., Grenha, A., Carrión-Recio, D., Seijo, B., Remuñán-López, C., 2012.  
560 Microencapsulated chitosan nanoparticles for pulmonary protein delivery: in vivo evaluation of  
561 insulin-loaded formulations. *J. Control. Release* 157, 383-390.
- 562 Andrews, G.P., Laverty, T.P., Jones, D.S., 2009. Mucoadhesive polymeric platforms for controlled  
563 drug delivery. *Eur. J. Pharm. Biopharm.* 71, 505-518.
- 564 Azevedo, J.R., Sizilio, R.H., Brito, M.B., Costa, A.M.B., Serafini, M.R., Araújo, A.A.S., Santos, M.  
565 R.V., Lira, A.A.M., Nunes, R.S., 2011. Physical and chemical characterization insulin-loaded  
566 chitosan-TPP nanoparticles. *J. Therm. Anal. Calorim.* 106, 685-689.
- 567 Bagre, A.P., Jain, K., Jain, N.K., 2013. Alginate coated chitosan core shell nanoparticles for oral  
568 delivery of enoxaparin: In vitro and in vivo assessment. *Int. J. Pharm.* 456, 31-40.
- 569 Berger, J., Reist, M., Mayer, J.M., Felt, O., Peppas, N.A., Gurny, R., 2004. Structure and  
570 interactions in covalently and ionically crosslinked chitosan hydrogels for biomedical applications.  
571 *Eur. J. Pharm. Biopharm.* 57, 19-34.
- 572 Bigucci, F., Luppi, B., Cerchiara, T., Sorrenti, M., Bettinetti, G., Rodriguez, L., Zecchi, V., 2008.  
573 Chitosan/pectin polyelectrolyte complexes: selection of suitable preparative conditions for colon-  
574 specific delivery of vancomycin. *Eur. J. Pharm. Sci.* 35, 435-441.
- 575 Blasi, P., Schoubben, A., Traina, G., Manfroni, G., Barberini, L., Alberti, P.F., Cirotto, C., Ricci,  
576 M., 2013. Lipid nanoparticles for brain targeting III. Long-term stability and in vivo toxicity. *Int. J.*  
577 *Pharm.* 454, 315-323.
- 578 Borges, O., Borchard G., Verhoef, J.C., Sousa, A., Junginger, H.E., 2005. Preparation of coated  
579 NPs for a new mucosal vaccine delivery systems. *Int. J. Pharm.*, 229, 155-166.
- 580 Borgogna, M., Bellich, B., Cesàro, A., 2011. Marine Polysaccharides in Microencapsulation and  
581 Application to Aquaculture: "From Sea to Sea". *Mar. Drugs* 9, 2572-2604.
- 582
- 583 Calvo, P., Remunan-Lopez, R., Vila-Jato, C.J.L., Alonso, M.J., 1997. Chitosan and  
584 chitosan/ethylene oxide-propylene oxide block copolymer NPs as novel carriers for proteins and  
585 vaccines. *Pharm. Res.* 14, 1431-1436.
- 586 Cesàro, A., Ciana, A., Delben F., Manzini, G., Paoletti, S., 1982. Physicochemical properties of  
587 pectic acid. I. Thermodynamic evidence of a pH-induced conformational transition in aqueous  
588 solution. *Biopolymers* 21, 431-449.
- 589 Derakhshandeh, K., Fathi, S., 2012. Role of chitosan nanoparticles in the oral absorption of  
590 Gemcitabine. *Int. J. Pharm.* 437, 172-177.

591 Desai, N., 2012. Challenges in development of nanoparticle-based therapeutics. *The AAPS journal*,  
592 14, 282-295.

593 Donati I., Stredanska, S., Silvestrini, G., Vetere, A., Marcon, P., Marsich, E., Mozetic, P., Gamini,  
594 A., Paoletti, S., Vittur, F., 2005. The aggregation of pig articular chondrocyte and synthesis of  
595 extracellular matrix by a lactose-modified chitosan. *Biomaterials* 26, 987-998.

596

597 Fazil, M., Md, S., Haque, S., Kumar, M., Baboota, S., Ali, J., 2012. Development and evaluation of  
598 rivastigmine loaded chitosan nanoparticles for brain targeting. *Eur. J. Pharm. Sci.* 47, 6-15.

599 Gonzalez-Mira, E., Egea, M.A., Garcia, M.L., Souto, E.B., 2010. Design and ocular tolerance of  
600 flurbiprofen loaded ultrasound-engineered NLC. *Colloids Surf. B Biointerfaces* 81, 412-421.

601 Goycoolea, F.M., Lollo, G., Remunan-Lopez, C., Quaglia, F., Alonso, M.J., 2009. Chitosan-  
602 alginate blended nanoparticles as carriers for the transmucosal delivery of macromolecules.  
603 *Biomacromolecules* 10, 1736-1743.

604 Hagesaether, E., Bye, R., Sande, S.A., 2008. Ex vivo mucoadhesion of different zinc-pectinate  
605 hydrogel beads. *Int. J. Pharm* 347, 9-15.

606 He, P., Davis, S.S., Illum, L., 1998. In vitro evaluation of the mucoadhesive properties of chitosan  
607 microspheres. *Int. J. Pharm.* 166, 75-68.

608 Knaul, J.Z., Hudson, S.M., Creber, K.A.M., 1999. Improved mechanical properties of chitosan  
609 fibers. *J. Appl. Polym. Sci.* 72, 1721-1731.

610 Marras-Marquez, T., Peña, J., Veiga-Ochoa, M.D., 2015. Robust and versatile pectin-based drug  
611 delivery systems. *Int. J. Pharm* 479, 265-276.

612 Mishra, R. K., Datt, M., Banthia, A. K., 2008. Synthesis and characterization of pectin/PVP  
613 hydrogel membranes for drug delivery system. *AAPS PharmSciTech* 9, 395-403.

614 Mouez, A., Zaki, N. M., Mansour, S., Geneidi, A. S., 2014. Bioavailability enhancement of  
615 verapamil HCl via intranasal chitosan microspheres. *Eur. J. Pharm. Sci.* 51, 59-66.

616 Nasti, A., Zaki, N.M., De Leonardis, P., Ungphaiboon, S., Sansongsak, P., Rimoli, M.G., Tirelli, N.,  
617 2009. Chitosan/TPP and chitosan/TPP-hyaluronic acid nanoparticles: systematic optimisation of the  
618 preparative process and preliminary biological evaluation. *Pharm. Res.* 26, 1918-1930.

619 Papadimitriou, S., Bikiaris, D., Avgoustakis, K., Karavas, E., Georgarakis, M., 2008. Chitosan  
620 nanoparticles loaded with dorzolamide and pramipexole. *Carbohydr. Polym.* 73, 44-54.

621 Rampino, A., Borgogna, M., Blasi, P., Bellich, B., Cesàro, A., 2013. Chitosan NPs: Preparation,  
622 size evolution and stability. *Int. J. Pharm.* 455, 219-228.

623 Sarmiento, B., Ferreira, D., Veiga, F., Ribeiro, A., 2006a. Characterization of insulin-loaded alginate  
624 nanoparticles produced by ionotropic pre-gelation through DSC and FTIR studies. *Carbohydr.*  
625 *Polym.* 66, 1-7.

- 626 Sarmiento, B., Martins, S., Ribeiro, A., Veiga, F., Neufeld, R., Ferreira, D., 2006b. Development  
627 and comparison of different nanoparticulate polyelectrolyte complexes as insulin carriers. *Int. J.*  
628 *Pept. Res. Ther.* 12, 131-138.
- 629 Saw, C.L.L., Heng, P.W.S., Liew, C.V., 2008. Chick chorioallantoic membrane as an in situ  
630 biological membrane for pharmaceutical formulation development: a review. *Drug Dev. Ind.*  
631 *Pharm.* 34, 1168-1177.
- 632 Schoubben, A., Blasi, P., Marenzoni, M.L., Barberini, L., Giovagnoli, S., Cirotto, C., Ricci, M.,  
633 2013. Capreomycin supergenerics for pulmonary tuberculosis treatment: preparation, in vitro, and in  
634 vivo characterization. *Eur. J. Pharm. Biopharm.* 83, 388-395.
- 635 Serra, L., Doménech, J., Peppas, N.A., 2009. Engineering design and molecular dynamics of  
636 mucoadhesive drug delivery systems as targeting agents. *Eur. J. Pharm. Biopharm.* 71, 519-528.
- 637 Shukla, S.K., Mishra, A. K., Arotiba, O.A., Mamba, B.B., 2013. Chitosan-based nanomaterials: A  
638 state-of-the-art review. *Int. J. Biol. Macromol.* 59, 46-58.
- 639 Sinha, V.R., Singla, A.K., Wadhawan, S., Kaushik, R., Kumria, R., Bansal, K., Dhawan, S., 2004.  
640 Chitosan microspheres as a potential carrier for drugs. *Int. J. Pharm.* 274, 1-33.
- 641 Sogias, I.A., Williams, A.C., Khutoryanskiy, V.V., 2012. Chitosan-based mucoadhesive tablets for  
642 oral delivery of ibuprofen. *Int. J. Pharm.* 436, 602-610.
- 643 Synytsya, A., Copikova, J., Matejka, P., Machovic, V., 2003. Fourier transform Raman and infrared  
644 spectroscopy of pectins. *Carbohydr. Polym.* 54, 97-106.
- 645 Vargas, A., Zeisser-Labouèbe, M., Lange, N., Gurny, R., Delie, F., 2007. The chickembryo and its  
646 chorioallantoic membrane (CAM) for the in vivo evaluation of drug delivery systems. *Adv. Drug*  
647 *Deliv. Rev.* 59, 1162-1176.
- 648 Woranuch, S., Yoksan, R., 2013. Eugenol-loaded chitosan nanoparticles: I. Thermal stability  
649 improvement of eugenol through encapsulation. *Carbohydr. Polym.* 96, 578-585.
- 650 Xu, Y., Du, Y., 2003. Effect of molecular structure of chitosan on protein delivery properties of  
651 chitosan nanoparticles. *Int. J. Pharm.* 250, 215-226.
- 652 Yu, C.Y., Yin, B.C., Zhang, W., Cheng, S.X., Zhang, X.Z., & Zhuo, R.X., 2009. Composite  
653 microparticle drug delivery systems based on chitosan, alginate and pectin with improved pH-  
654 sensitive drug release property. *Colloids Surf. B Biointerfaces* 68, 245-249.  
655

656 **CAPTION TO FIGURES:**

657 **Fig. 1:** mean size (a) and Z-potential (b) of chitosan NPs (chitosan:TPP ratio 5:1 w/w) coated with  
658 sodium polygalacturonate (■), pectin from citrus fruit (●) and pectin from apple (▲).  
659

660 **Fig. 2:** mean size of chitosan NPs blended with apple pectin in different ratios with TPP. Ratio  
661 pectin:TPP 1:1 (■), 2:1 (●), 4:1 (▲), 6:1 (▼) and 8:1 (◆). The mean size of NPs in the absence of  
662 pectin is in the range of 200 nm.

663  
664 **Fig. 3:** FTIR spectra of a) chitosan (dash line) and chitosan NPs (full line); b) chitosan NPs (black  
665 full line), polygalacturonate (red dash line), polygalacturonate coated NPs (blue full line); c)  
666 chitosan NPs (black full line), apple pectin (red dash line), apple pectin coated NPs (blue full line)  
667 and apple pectin blended NPs (blue dot line); d) chitosan NPs (black full line), citrus fruit pectin  
668 (red dash line), citrus fruit pectin coated NPs (blue full line).

669  
670 **Fig. 4:** DSC curves of a) chitosan (dash line) and chitosan NPs (straight line); b) apple pectin (dash  
671 line), coated NPs (straight line) with pectin and blended NPs (dot line) with pectin; c) citrus fruit  
672 pectin (dash line) and coated NPs (straight line) with pectin.

673  
674 **Fig. 5:** Chicken embryos at different stages of development observed during acute toxicity  
675 experiments. a, embryo before treatment; a', after material (apple pectin) deposition; a" after 24  
676 hours - b, embryo before treatment; b', after material (chitosan) deposition; b" after 24 hours - c,  
677 embryo before treatment; c', after material (chit/pect NPs) deposition; c" after 24 hours - d, embryo  
678 before treatment; d', after material (chit NPs) deposition; d" after 24 hours - e, embryo before  
679 treatment; e', after saline deposition (negative control); e" after 24 hours - f, embryo before  
680 treatment; f', after material ( $\lambda$  carrageenan) deposition (positive control); f" after 24 hours.

681  
682  
683  
684